

Wapl antagonizes cohesin binding and promotes Polycomb-group silencing in *Drosophila*

Melissa D. Cunningham¹, Maria Gause², Yuzhong Cheng¹, Amanda Noyes¹, Dale Dorsett², James A. Kennison¹ and Judith A Kassiss^{1,*}

SUMMARY

Wapl protein regulates binding of the cohesin complex to chromosomes during interphase and helps remove cohesin from chromosomes at mitosis. We isolated a dominant mutation in *wapl* (*wapl*^{4G}) in a screen for mutations that counteract silencing mediated by an *engrailed* Polycomb-group response element. *wapl*^{4G} hemizygotes die as pharate adults and have an extra sex combs phenotype characteristic of males with mutations in Polycomb-group (PcG) genes. The *wapl* gene encodes two proteins, a long form and a short form. *wapl*^{4G} introduces a stop codon at amino acid 271 of the long form and produces a truncated protein. The expression of a transgene encoding the truncated Wapl-AG protein causes an extra-sex-comb phenotype similar to that seen in the *wapl*^{4G} mutant. Mutations in the cohesin-associated genes *Nipped-B* and *pds5* suppress and enhance *wapl*^{4G} phenotypes, respectively. A Pds5-Wapl complex (releasin) removes cohesin from DNA, while Nipped-B loads cohesin. This suggests that Wapl-AG might exert its effects through changes in cohesin binding. Consistent with this model, Wapl-AG was found to increase the stability of cohesin binding to polytene chromosomes. Our data suggest that increasing cohesin stability interferes with PcG silencing at genes that are co-regulated by cohesin and PcG proteins.

KEY WORDS: Cohesin, Polycomb, Gene expression

INTRODUCTION

Control of gene expression is vital to normal development. During *Drosophila* development, spatially and temporally restricted DNA-binding transcriptional activators or repressors establish early patterns of gene expression. Later, two groups of genes, the trithorax group (*trxG*) and the Polycomb group (PcG) are responsible for maintaining gene expression throughout development (Kennison, 1995). The PcG genes encode a group of transcriptional repressors that act in protein complexes to modify chromatin (reviewed by Simon and Kingston, 2009; Kerppola, 2009; Müller and Verrijzer, 2009). One hallmark of PcG function is the histone modification, H3K27me3, specified by the PcG protein complex PRC2. The *trxG* genes were identified by their ability to counteract the action of PcG genes (Kennison, 1995). Most *trxG* genes encode subunits of complexes that activate transcription through chromatin modification or remodeling. However, important for this study, the *trxG* gene *verthandi* (*vtd*) encodes the cohesin subunit Rad21 (Hallson et al., 2008).

Cohesin is made up of the proteins Smc1, Smc3, Rad21 and Stromalin (SA), and is important for sister chromatid cohesion and proper chromosome segregation during mitosis. In addition, cohesin and cohesin-associated proteins play an important role in regulating gene expression (reviewed by Peters et al., 2008; Xiong and Gerton, 2010; Dorsett, 2011). In a recent study, the cohesin subunits Smc1, Smc3 and Rad21 were found to co-purify with the PcG protein Polycomb (Strübbe et al., 2011), suggesting these protein complexes may physically interact at some loci.

In *Drosophila*, PcG proteins act through DNA elements called Polycomb group response elements (PREs) (reviewed by Müller and Kassiss, 2006; Ringrose and Paro, 2007). In genome-wide studies, PREs are recognized as DNA fragments that are binding sites for multiple PcG proteins. The function of PREs can be tested in reporter assays in transgenic flies. One hallmark of PRE activity is their ability to repress the expression of the mini-*white* reporter gene, a commonly used marker for transgenic flies. The amount of repression is dependent on the number of PREs: more PREs equals more repression. Because PcG protein complexes interact with each other, this increase in repression is most likely due to an increase in the number or composition of PcG protein complexes that cooperate to repress or silence transcription. Homologous chromosomes are paired in *Drosophila*, and regulatory DNA on one chromosome can influence the expression of a gene on the homologous chromosome. Thus, PcG complexes bound to PRE-mini-*white* transgenes inserted near each other on homologous chromosomes can interact to silence the expression of the mini-*white* gene. This phenomenon is called pairing-sensitive repression or silencing (Kassiss, 1994). Because pairing-sensitive silencing is mediated by PREs, it is reasonable to assume it depends on PcG function. In fact, mutations in some PcG genes suppress pairing-sensitive silencing (reviewed by Kassiss, 2002).

In an effort to identify genes that are important for PcG silencing, particularly those that mediate interactions between PREs, we conducted a screen for dominant suppressors of pairing-sensitive silencing mediated by an *engrailed* PRE (Noyes et al., 2011). Here, we identify one of the suppressors we obtained in that screen as a mutation in the *wapl* gene, an unusual allele we named *wapl*^{4G}. Wapl is a cohesin-associated protein important for removing cohesin from chromosomes (Gandhi et al., 2006; Kueng et al., 2006; Shintomi and Hirano, 2009; Sutani et al., 2009; Gause et al., 2010). *wapl*^{4G} produces a truncated Wapl protein that acts in a dominant fashion to suppress pairing-sensitive silencing. Furthermore, *wapl*^{4G} pharate adults have an extra sex combs

¹Program in Genomics of Differentiation, Eunice Kennedy Shriver National Institute of Child Health and Human Development, National Institutes of Health, Bethesda, MD 20892, USA. ²Edward A. Doisy Department of Biochemistry and Molecular Biology, St Louis University School of Medicine, St Louis, MO 63104, USA.

*Author for correspondence (jk14p@nih.gov)

phenotype characteristic of mutations in PcG genes. Production of the truncated Wapl^{AG} protein in an otherwise wild-type background recapitulates the extra sex combs phenotype seen in the *wapl*^{AG} mutant and increases the stability of cohesin binding to polytene chromosomes. Our data suggest that increasing cohesin stability interferes with PcG silencing at genes that are co-regulated by cohesin and PcG proteins.

MATERIALS AND METHODS

Antibody production and immunostaining

Rabbit polyclonal antibodies (Covance) were raised against HIS-tag Wapl polypeptides that were purified with a HIS-affinity column (Enzymax). Polypeptide specific for Wapl-L was made from amino acids 1 to 300 and was used as the antigen to generate the α -Wapl-L antibody. The α -Wapl-SL antibody was generated against a polypeptide for amino acids 650 to 947 of Wapl-L (amino acids 1 to 300 of Wapl-S). Antibodies were affinity purified with the same polypeptide used for antibody production (Enzymax). For embryo immunoperoxidase staining, a 1:2500 dilution of crude anti-sera was used for both α -Wapl-SL and α -Wapl-L, according to standard procedures (Kwon et al., 2009). Similar results were obtained when using affinity-purified anti-sera (at a 1:50 dilution). Staining of polytene chromosomes was carried out using standard procedures (Eissenberg, 2006) with the following primary antibody dilutions: affinity-purified α -Wapl-L and α -Wapl-SL (1:20); α -Rad21 (1:100) and α -HA (1:800).

Western blots

Embryos overexpressing Wapl-L and Wapl-S were collected from UAS-Wapl-L and UAS-Wapl-S crossed to *en-Gal4*. For larval samples, ten 3rd instar larvae were cut in half and the anterior region was inverted to remove its trachea, salivary gland and gut. The remaining tissues were homogenized in lysis buffer (1× PBS, 1% Triton X-100, 1 mM MgCl₂, 5 mg/ml RNase A, 5 mg/ml DNase, 1× Halt Protease Inhibitor (Thermo Scientific), 5 mM EDTA). The homogenate was centrifuged at 15,000 g for 10 minutes at 4°C. The supernatant was transferred to a new tube and mixed with equal volume of 2× SDS sample buffer, boiled for 5 minutes, then chilled on ice prior to loading on gel. Proteins were separated in 4–15% Mini-Protein TGX gels (Biorad). The ECL Plus Western Blotting Detection System (GE Healthcare) was used. Antibody dilutions were 1:1000 affinity-purified α -Wapl-L and α -Wapl-SL.

Construction of UAS lines

UAS-Wapl-S

A partial *wapl* cDNA (LD16461) that contains the 5' end of the large *wapl* cDNA to a *XhoI* site was obtained from *Drosophila* Genomic Resource Center. The 5'-end fragment of the Wapl-S cDNA was generated by PCR with LD16461 as template and two primers (GTCAGTCGGCCG-ATGATGATGACCATCGACGGAGC and GTCAGTCGGCCGCTCG-AGGAAGCGTCCGTGT). This PCR product was ligated into pCRII-Blunt-TOPO vector (Invitrogen) then transferred from the TOPO vector into pUAST vector by *EagI* digestion, resulting in pUAST-Wapl-S-5'. To make the *wapl* 3'-end cDNA fragment, PCR was carried out on genomic DNA from the iso-1 *Drosophila* strain with two primers (CAAGGT-ACTGATCAACCTGACG and ACGTACTCGAGGTAAACGTACACATATA). The PCR fragment was ligated into pCRII-Blunt-TOPO vector. This plasmid was cut with *XhoI* to obtain the *wapl* 3'-end fragment, which was ligated into *XhoI*-digested pUAST-Wapl-S-5'. Recombinant clones with the right orientation of the *wapl* 3'-end fragment were identified by *EcoRI* digestion. The final construct, pUAST-Wapl-S, was verified by DNA sequencing.

UAS-Wapl-L

PCR was carried out with LD16461 as template and two primers (GTCAGTAGATCTATGTCGCGCTGGGGCAAGAA and a 3' primer downstream of the *BglII* site). This PCR fragment was ligated into pCRII-Blunt-TOPO. The *wapl*-L-5' fragment was released from this clone by *BglII* digestion and ligated into *BglII*-digested pUAST-Wapl-S backbone. The right clone was identified by PCR and DNA digestion with *PstI*. The final plasmid pUAST-Wapl-L was sequenced to confirm its identity.

pUAST-Wapl-AG

The *wapl*^{AG} cDNA was generated by PCR with pUAST-Wapl-L as template. The two PCR primers are CAGAGATCTATGTCGCGCTG-GGGCAAGA (with an added *BglII* site), and CATCTCGAGTTAGCGC-CCCGCTTTGGGA (which has an added *XhoI* site and introduces the *wapl*^{AG} stop codon). The PCR product was digested with *BglII* and *XhoI* and ligated into the *BglII* and *XhoI* cut pUAST vector. Recombinant clones were selected and the *wapl*^{AG} cDNA insert was sequenced.

UAS-Wapl-AG-HA

The *wapl*^{AG} cDNA was generated by PCR with primers CACCATGT-CGCGCTGGGGCAAGA and GCGCCCCGCTTTGGGAATG using pUAST-Wapl-L as template. The PCR product was ligated into pENTR-D-TOPO vector (Invitrogen). Plasmid from the recombinant clones was then transferred into the pTWH vector (developed by T. Murphy's lab, Baltimore, MD; <http://emb.carnegiescience.edu/labs/murphy/Gateway%20vectors.html>) with Gateway LR Clonase Enzyme Mix (Invitrogen). The final construct was named pTWH-*wapl*^{AG} and its *wapl*^{AG} cDNA insert was verified by DNA sequencing. Transgenic lines were made using standard techniques (Genetics Services and BestGene).

Fluorescence recovery after photobleaching

FRAP was conducted with late 3rd instar salivary glands of the indicated genotypes as previously described using an EGFP-Smc1 expressing transgene (Gause et al., 2010). This transgene uses the *Chip* gene promoter to express EGFP-Smc1 at lower levels than endogenous Smc1. EGFP-Smc1 rescues *Smc1* null mutants to pharate adulthood and is incorporated into cohesin (Gause et al., 2010).

Rescue experiments

y wapl^{AG} *w UAS-Wapl-S/FM0* virgin females were crossed to *arm-Gal4* homozygous males. Progeny were 14 males of the genotype *y wapl*^{AG} *w UAS-Wapl-S*; *arm-Gal4*^{+/+}; 50 *FM0*; *arm-Gal4*^{+/+} males; 51 *FM0*^{+/+}; *arm-Gal4*^{+/+} females; and 49 *y wapl*^{AG} *w UAS-Wapl-S*^{+/+}; *arm-Gal4*^{+/+} females (14 rescued males out of 50 expected). We did not obtain any rescued males from a similar cross of *y wapl*^{AG} *w UAS-Wapl-L/FM0* virgin females to *arm-Gal4* males (about 300 progeny scored). Because the UAS-Wapl-L was inserted in a different chromosomal location than UAS-Wapl-S, we do not know whether the lack of rescue with UAS-Wapl-L is the result of either too much or too little Wapl-L protein made from this insertion site, or from a difference in the activity of the two proteins. Similar crosses with *wapl*² showed that neither UAS-Wapl-S nor UAS-Wapl-L could rescue this null mutant.

Non-disjunction

To generate germline clones, *y wapl*^{AG} *w P{FRT(w^{hs})}101/FM0* or *y^l w v²⁴ P{FRT(w^{hs})}101* virgin females were crossed to *w ovo*^{D1} *v²⁴ P{FRT(w^{hs})}101/Y*; *P{hsFLP}38* males. After 1 day, parents were removed. The larvae were aged for 1 day and then heat-shocked at 37°C for 1 hour on two consecutive days (Chou and Perrimon, 1996). Virgin females of the genotypes *y wapl*^{AG} *w P{FRT(w^{hs})}101/w ovo*^{D1} *v²⁴ P{FRT(w^{hs})}101* and *y^l w v²⁴ P{FRT(w^{hs})}101 /wovo*^{D1} *v²⁴ P{FRT(w^{hs})}101* were crossed to *C(4)RM, ci ey*^{R/O}. Non-disjunction and chromosome loss were detected as *y*⁺ sons (X chromosome non-disjunction and loss) and *ci ey* progeny (4th chromosome non-disjunction and loss).

RESULTS

Molecular characterization of *wapl* alleles

We conducted a screen for dominant suppressors of pairing-sensitive silencing by a 181 bp *engrailed* PRE and recovered nine mutants (Noyes et al., 2011). One of the dominant suppressors mapped to the X chromosome and was hemizygous and homozygous lethal. We mapped the mutation between *y* and *w* by recombination mapping. We then used small deficiencies and gene-specific mutations to determine that the mutation was in the *wapl* gene, and named the allele *wapl*^{AG}. The *wapl* gene encodes two transcripts, a large transcript and a small transcript, generating a large and small protein – Wapl-L and Wapl-S (Fig. 1). The

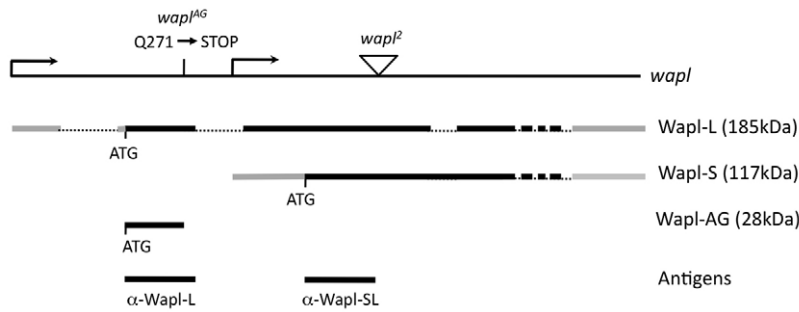


Fig. 1. *wapl* transcripts, mutations and proteins. (A) Top black line is *wapl* DNA. Large and small *wapl* transcripts are produced from independent transcription start sites (arrows). The two transcripts encoding Wapl-L and Wapl-S are shown. Exons are thick lines (gray, non-coding; black, coding). Introns are dotted lines. Locations of the *wapl*^{L2} and *wapl*^{AG} mutations are shown. Sequencing of *wapl*^{L2} mutants identified an insertion of 970 bases from the *Egf* gene normally found on chromosome 2R. The *wapl*^{AG} mutation consists of a single nucleotide change of C to T at position 1583 of the cDNA sequence. The antigens used to generate the two antibodies and the predicted sizes of the three Wapl proteins discussed in this paper are also shown.

transcription start site for the small transcript is within an intron of the large transcript (McQuilton et al., 2012). The large transcript codes for a protein of 1741 amino acids; *wapl*^{AG} is a nonsense mutation at Gln²⁷¹ (CAA to TAA) of the large protein. This suggests that it truncates Wapl-L protein but does not interfere with the production of Wapl-S. In addition, we determined the molecular lesion of *wapl*^{L2}, the null mutation we used in our experiments. *wapl*^{L2} was reported to contain an insertion of about 1.6 kb of DNA into the middle of the *wapl* gene, eliminating the correct production of both the large and small *wapl* mRNA transcripts (Verni et al., 2000). We determined that *wapl*^{L2} contains a 970 bp insertion of DNA from the epidermal growth factor receptor gene into an exon common to both the large and small proteins, and eliminates the production of both proteins (see below).

The sequence similarity between *Drosophila* Wapl and human, *C. elegans* and yeast Wapl proteins is contained within the C-terminal region of the *Drosophila* proteins, extending from amino acids 488 to 1018 of the short protein and amino acid 1137 to 1667 of the long protein (Kueng et al., 2006). We examined the sequence conservation of the 649 amino acids unique to the long protein. The entire 649 amino acids are well conserved in the genus *Drosophila* (data not shown). In addition, ~100 amino acids at the N terminus are conserved in all insects (data not shown) but not in other organisms. This suggests that this part of the protein has an important function in insects.

***wapl*^{AG} is a gain-of-function mutation**

wapl^{AG} suppresses pairing-sensitive silencing of *mini-white* by a 181 bp PRE (Fig. 2). *wapl*^{AG} *w*/*FM0*; *P*[181PRE]8-10C/*P*[181PRE]8-10C flies have yellow eyes (similar to what was seen with our other suppressors), whereas *w*; *P*[181PRE]8-10C/*P*[181PRE]8-10C have white eyes. Interestingly, *wapl*^{L2} *w*/*FM0*; *P*[181PRE]8-10C/*P*[181PRE]8-10C also have white eyes, showing that loss of one copy of *wapl* is not sufficient to generate the phenotype observed (data not shown). This shows that *wapl*^{AG} is a gain-of-function mutation. *wapl*^{AG}, unlike the other dominant suppressors of pairing-sensitive silencing that we isolated (Noyes et al., 2011), has no effect on the heterozygous eye color of *P*[181PRE]8-10C. This suggests that *wapl*^{AG} may interfere with the interaction between PREs, which enhances the silencing activity of these elements.

Given the molecular nature of the *wapl*^{AG} mutation, we reasoned that the gain-of-function phenotype could be due to either the

production of a truncated protein, or to a disruption in the ratio of Wapl-S versus Wapl-L protein. We therefore generated antibodies to Wapl to test whether *wapl*^{AG} could generate a stable protein.

***wapl*^{AG} produces a truncated protein**

We generated rabbit antibodies against two antigens: one specific for the large protein (α-Wapl-L) and one that will detect both the small and the large proteins (α-Wapl-SL) (Fig. 1). Western blots show the specificity of α-Wapl-L for the large protein, whereas α-Wapl-SL detects two bands (Fig. 3). Both Wapl proteins are present in embryos at similar levels, whereas the predominant form in larvae is Wapl-L (Fig. 3B,C). This is consistent with RNA-seq data that shows that the Wapl small transcript is expressed at a very low level in larvae (McQuilton et al., 2012). The western blots also show the complete absence of both Wapl proteins in *wapl*^{L2} larvae, and the absence of Wapl-L in *wapl*^{AG} larvae (Fig. 3C). Both antibodies detect nuclear antigens in embryos (Fig. 3D-G).

Interestingly, α-Wapl-L detects a protein of about 30 kDa in *wapl*^{AG} embryos (Fig. 3A) and larvae (supplementary material Fig.



Fig. 2. Suppression of pairing-sensitive silencing in *wapl*^{AG} mutants. Wild-type flies homozygous for *w*; *P*[181PRE]8-10C have white eyes (left), whereas *wapl*^{AG} *w*/*FM0*; *P*[181PRE]8-10C flies have a light-orange eye color (right). The eye color of *wapl*^{AG} *w*/*FM0*; *P*[181PRE]8-10C was similar to that seen in a number of the mutants we obtained in our screen for dominant suppressors of pairing-sensitive silencing.

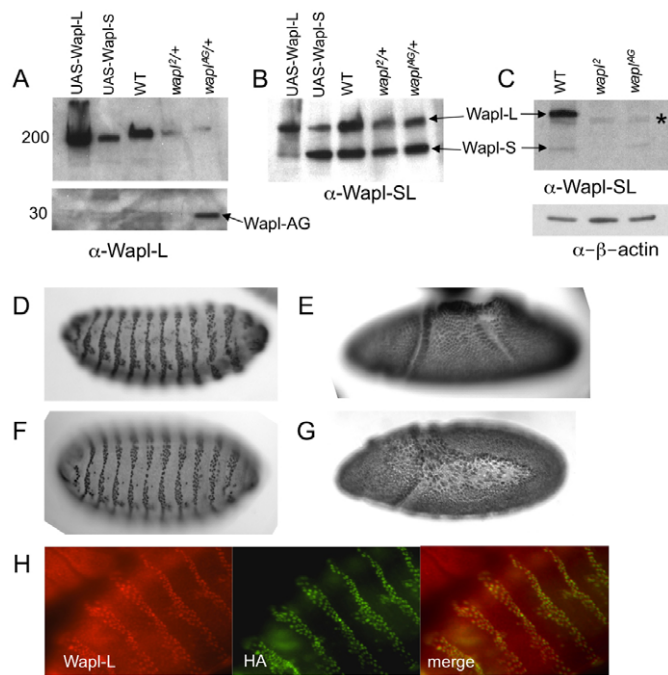


Fig. 3. Wapl-L, Wapl-S and Wapl-AG are nuclear proteins.

(A–C) Western blots using the α-Wapl-L (A) (specific for Wapl-L) and α-Wapl-SL (B,C) (the antibody reacts with both Wapl-S and Wapl-L) on embryonic (A,B) and larval (C) crude protein extracts. (A) Numbers on left show approximate molecular weights. (A,B) The identity of Wapl-L (upper band) or Wapl-S (lower band) is confirmed by overexpression of UAS-Wapl-L or UAS-Wapl-S by an *arm*-Gal4 driver. (A, lower panel) Western blot probed with α-Wapl-L detected an additional band in *wapl^{AG}/+* embryos running about 30 kDa, close to the predicted size of a truncated Wapl-AG protein (28.6kDa). (C) An asterisk indicates the location of a crossreacting band in larval extracts (lower panel). The blot was reprobed with α-β-actin for a loading control. (D–G) Embryos stained with Wapl antibodies. Embryos overexpressing UAS-Wapl-L or UAS-Wapl-S from an *engrailed*-Gal4 driver (D,F) and wild-type embryos (E,G) were stained with either α-Wapl-L (D,E) or α-Wapl-SL (F,G). Engrailed-stripped staining pattern shows specific nuclear staining of overexpressed Wapl proteins by the Gal4 driver. Wild-type embryos showed ubiquitous nuclear staining at all embryonic stages (except in mitotic nuclei, not shown) when stained with either α-Wapl-L or α-Wapl-SL. Embryos anterior leftwards, dorsal upwards. (D,F) Stage 15, (E) stage 8 and (G) stage 9. Native Wapl protein is present at a much lower level than the UAS-driven Wapl proteins. Pictures of wild-type embryos were taken with a longer exposure time than the UAS-Wapl embryos. (H) Wapl-AG is a nuclear protein. UAS-Wapl-AG-HA driven by *engrailed*-Gal4 is detected in embryos by staining with α-Wapl-L and α-HA. α-Wapl-L also reacts with endogenous Wapl-L (note red embryo in upper left corner not stained by α-HA).

S1), but not in wild-type embryos. The expected molecular weight for the truncated mutant protein is 28 kDa. In order to test whether this protein is also nuclear, we made a UAS-Wapl-AG construct encoding the predicted truncated mutant protein and expressed it under the control of *engrailed*-Gal4 so that the protein would be expressed in stripes in embryos (Fig. 3H). Two versions of UAS-Wapl-AG were made, one HA-tagged to distinguish the ectopic protein from wild-type Wapl-L and one without a tag. Both Wapl-AG and Wapl-AG-HA are nuclear proteins (Fig. 3H and data not shown).

Wapl colocalizes with cohesins on polytene chromosomes

Wapl plays an important role in removing cohesins from chromosomes for cell division, and regulates cohesin chromosome-binding dynamics during interphase, but its role in gene expression has not been explored. Similar to its interaction partner Pds5, we found that Wapl colocalizes with Rad21 and Nipped-B on polytene chromosomes (Fig. 4 shows Rad21 colocalization). No Wapl protein was seen with either the α-Wapl-L or the α-Wapl-SL antibodies on *wapl²* polytene chromosomes, confirming the specificity of our antibodies (supplementary material Fig. S2 and data not shown). In addition, we observed that Rad21 and Nipped-B were both bound to polytene chromosomes in the absence of Wapl (data not shown), consistent with *in vivo* fluorescence recovery after photobleaching (FRAP) experiments (Gause et al., 2010). Wapl-AG-HA binds to the same bands as Rad21, as well as to additional bands (Fig. 4B). We suggest that Wapl-AG could be mediating its phenotypic effects via an interaction with cohesin.

The *wapl^{AG}* mutant phenotype is caused by the production of the truncated Wapl^{AG} protein

wapl² mutants die at the larval-pupal boundary and have small imaginal discs (Verni et al., 2000). Although most *wapl^{AG}* mutants die during the pupal stage without the development of cuticle, a few make it to pharate adults. We examined the phenotype of *wapl^{AG}* hemizygous males and found they have an extra sex combs phenotype that is characteristic of males with mutations in PcG genes (Fig. 5A). We suspected that this phenotype might be due to the truncated Wapl-AG protein. In fact, overexpression of UAS-Wapl-AG or UAS-Wapl-AG-HA by the *daughterless*-Gal4 driver caused an extra sex combs phenotype (Fig. 5B). In addition, several other phenotypes were observed with overproduction of Wapl-AG or Wapl-AG-HA: extra and abnormal sternopleural bristles (Fig. 5C), a failure in dorsal-ventral fusion in the most posterior abdominal segment (Fig. 5D) and twisted genitalia (Fig. 5B). UAS-Wapl-AG or UAS-Wapl-AG-HA inserted in different chromosomal insertion sites showed similar phenotypes, but to different extents (Table 1). This probably reflects a difference in expression levels of the transgenes. Extra sternopleural bristles and a failure in dorsal-ventral fusion were also observed in some *wapl^{AG}* pharate adults (data not shown). Overexpression of Nipped-B greatly reduces viability, but surviving adults display a failure in dorsal-ventral fusion (Fig. 5E) and twisted genitalia (not shown), similar to phenotypes seen by Wapl-AG. Similar to Wapl-AG (see below), overexpression of Nipped-B increases the stability of cohesin binding to polytene chromosomes (Gause et al., 2010).

wapl^{AG} interacts with *pds5* and *Nipped-B* mutations and increases the stability of cohesin binding to polytene chromosomes

We examined the effect of mutations in the genes *pds5* and *Nipped-B* on the suppression of pairing-sensitive silencing by *wapl^{AG}* and the extra sex combs phenotype seen in *UAS-Wapl-AG-HA*; *da-GAL4* males. Pds5 forms the releasin complex with Wapl to unload cohesin from the chromosome, whereas Nipped-B complexes with the Mau-2 protein to form the kollerin complex that loads cohesin (Nasmyth, 2011). The heterozygous null *pds5^{5e3}* mutation further darkened the *wapl^{AG} w/w*; *P[181PRE]8-10C* eye color, whereas *Nipped-B²⁹* lightened it (Fig. 6A). Furthermore, heterozygous mutations in *Nipped-B* suppressed and *pds5* enhanced the extra sex combs phenotype seen in *UAS-Wapl-AG-HA*; *da-GAL4* flies (Fig. 6B). It has been shown that heterozygous *pds5^{5e3}* increased the

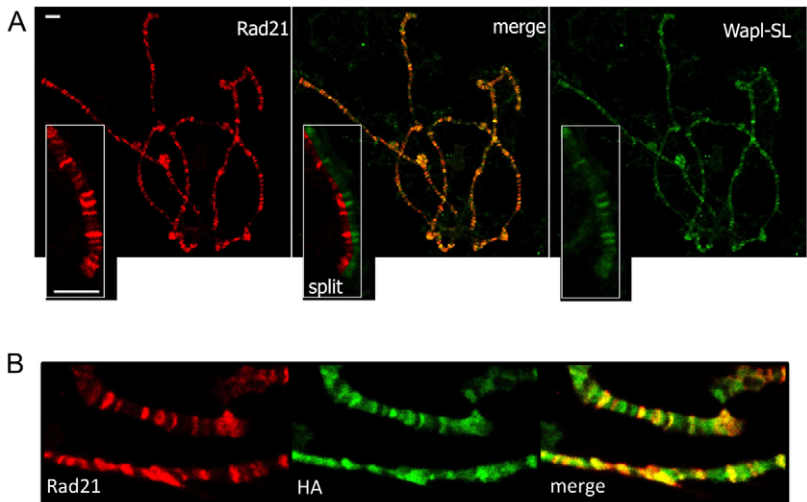


Fig. 4. Wapl proteins colocalize with the cohesin subunit Rad21 on polytene chromosomes. (A) All panels include a picture of an entire genome and an enlargement of a small region (insets). Scale bar: 10 μ m. As there is very little Wapl-S in larvae (see Fig. 3), these pictures reflect the distribution of Wapl-L on the polytene chromosomes. (B) Wapl-AG-HA binds to polytene chromosomes. A small region of the genome is shown. Wapl-AG-HA co-localizes with Rad21 but also binds more broadly to polytene chromosomes.

amount of stable cohesin binding to salivary chromosomes, and a heterozygous *Nipped-B* mutation decreased the amount of stable cohesin (Gause et al., 2010). Because Wapl is thought to act with Pds5 to remove cohesin, we predicted that Wapl-AG would increase the stability of cohesin binding. The dynamics of cohesin binding were compared in *EGFP-Smc1/+; da-GAL4/+* control and *EGFP-Smc1/UAS-Wapl-AG-HA; da-GAL4* salivary glands using FRAP to determine the effects of Wapl-AG on cohesin binding

(Fig. 7). As before, we found cohesin in three pools: unbound, weak and strong binding (Gause et al., 2010). Wapl-AG increases the half-life of the stably bound population threefold (from 237 to 772 seconds) without affecting the half-life of the weakly bound population. Furthermore, the amount of stably-bound cohesin increased two-fold in *UAS-Wapl-AG-HA; da-GAL4* polytenes, from 13% to 26% of the total cohesin population. This increase in cohesin stability was similar to that seen in the loss-of-function *wapl²* hemizygotes. We suggest that Wapl-AG interferes with the unloading of cohesins from the chromosome causing an increase in binding stability. A decrease in the amount of Pds5 further increases stable cohesin leading to enhanced phenotypes, whereas a decrease in the amount of *Nipped-B* reduces cohesin loading and alleviates the *wapl^{AG}* phenotypes.

What causes the lethality of *wapl^{AG}*?

We used UAS-Wapl-S and UAS-Wapl-L in an attempt to rescue the lethality of *wapl^{AG}*. We found that driving the expression of UAS-Wapl-S and UAS-Wapl-L by the *da-GAL4* driver caused lethality in both wild-type and *wapl^{AG}* flies. Therefore, we used the *arm-GAL4* driver and observed that UAS-Wapl-S could rescue the lethality of *wapl^{AG}* (see Materials and methods for details). Some of the rescued *wapl^{AG}* males looked phenotypically normal, showing that Wapl-S could rescue the phenotypes normally seen in *wapl^{AG}* males. Our results suggest that both the lethality and the

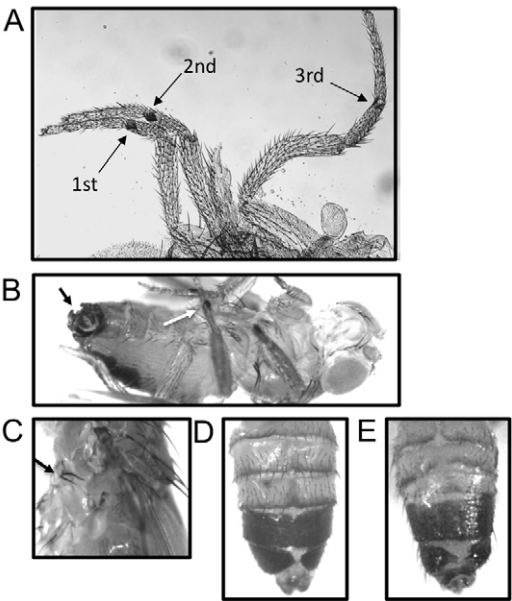


Fig. 5. Wapl-AG causes extra sex comb teeth and other phenotypes. (A) This *wapl^{AG}* pharate adult male has sex comb teeth on all three legs (arrows). The 2nd leg has eight sex comb teeth, the third leg has two sex comb teeth. (B–D) UAS-Wapl-AG-HA driven by the *da-Gal4* driver produces flies with (B) a complete sex comb on the 2nd leg (white arrow) and twisted genitalia (black arrow), (C) abnormal sternopleural bristles (arrow), and (D) defects in dorsal-ventral fusion in the most posterior abdominal segment. (E) The abdomen of a *da-Gal4/+; UAS-Nipped-B/+* male. The abnormal sternopleural bristles could be caused by mis-expression of *wingless*, a PcG-regulated gene. The abdominal phenotype and twisted genitalia could be caused by mis-regulation of *Abd-B*, also a PcG-regulated gene.

Table 1. Phenotypes seen in UAS-Wapl-AG inserted at different insertion sites

Line name	Chromosome*	Cross to <i>da-Gal4</i> ‡
UAS-Wapl-AG-2	3	P, Sp
UAS-Wapl-AG-1	3	Early pupal lethal
UAS-Wapl-AG-8	3	Pharate lethal, esc [§]
UAS-Wapl-AG-7	3	P, Sp
UAS-Wapl-AG-HA-5	3	P
UAS-Wapl-AG-HA-4	3	P, Sp, esc
UAS-Wapl-AG-HA-2	2	P, Sp, esc
UAS-Wapl-AG-HA-6	2	P, Sp

*Chromosome transgene is inserted on.
‡Phenotypes observed: P, defects in posterior abdomen; Sp, abnormal or extra sternopleural bristles; esc, sex comb teeth on the second leg.
§Sex comb teeth on the second legs were observed through the pupal case. We did not dissect the pharate adults to look for the other phenotypes.

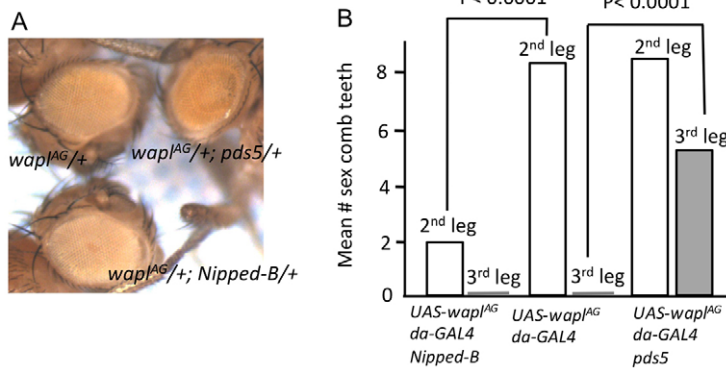


Fig. 6. *pds5* enhances and *Nipped-B* suppresses the *wapl*^{AG} phenotypes. (A) All flies are homozygous for *w* and *P[181PRE]8-10C* in addition to the mutations shown. *wapl*^{AG} *w/w*; *P[181PRE]8-10C/P[181PRE]8-10C* flies have light orange eyes; *wapl*^{AG} *w/w*; *Nipped-B*²⁹ *P[181PRE]8-10C/P[181PRE]8-10C* flies have white eyes; *wapl*^{AG} *w/w*; *pds5*^{es3} *P[181PRE]8-10C/P[181PRE]8-10C* flies have orange eyes. Neither *Nipped-B*²⁹ nor *pds5*^{es3} alters the eye color of *P[181PRE]8-10C* flies in the absence of the *wapl*^{AG} mutation (not shown). (B) Mean numbers of sex comb teeth on the 2nd and 3rd legs of flies heterozygous for the indicated genotypes. Sex comb teeth on 26 legs from each genotype were counted. As *UAS-Wapl-AG*; *da-Gal4/pds5*^{es3} flies die as pharate adults, flies were dissected from pupal cases prior to counting sex comb teeth.

abnormal phenotypes seen in *wapl*^{AG} mutants are caused by a decrease in Wapl function and that the truncated Wapl^{AG} protein interferes with the normal function of Wapl.

wapl^{AG} produces half of the N terminus of Wapl-L (the location of most of the insect-conserved amino acids), and *wapl*^{AG}; *UAS-Wapl-S*; *arm-Gal4* rescued flies would have both Wapl-S and Wapl-AG. Therefore, we cannot conclude that the N terminus of Wapl is dispensable for viability in flies. Attempts to rescue *wapl*^{AG} by *UAS-Wapl-L* or *wapl*² by *UAS-Wapl-L* and *UAS-Wapl-S* were not successful (for details see Materials and methods). We suspect this could have been due to difficulties obtaining the correct level of expression of the transgenes.

Embryos that lack maternal Wapl proteins, generated by making germline clones in *wapl*² heterozygous mothers, arrest before the cellular blastoderm stage with many abnormal nuclei (Perrimon et al., 1985; and data not shown). By contrast, embryos derived from maternal germline clones of *wapl*^{AG} can be paternally rescued by a wild-type *wapl* allele. The *wapl*^{AG} zygotic mutants from these maternal germline clones die at the same stage as *wapl*^{AG} zygotic mutants from heterozygous mothers. Wapl-S proteins expressed from the *wapl*^{AG} mutant chromosome must be sufficient to rescue the early embryonic requirement for *wapl* function. Females heterozygous for *wapl* mutations show an increase in non-disjunction (Verni et al., 2000). Therefore, we examined non-disjunction of the X and 4th chromosome from the germline clones of *wapl*^{AG}. Like other *wapl* mutants, *wapl*^{AG} causes an increase in non-disjunction (Table 2). All of our results suggest that *wapl*^{AG} reduces the amount of functional Wapl protein, leading to zygotic lethality, extra sex comb teeth in males and non-disjunction in oocytes.

DISCUSSION

Our results suggest a role for the cohesin-associated protein Wapl in the control of gene expression and regulation of PcG silencing at genes co-regulated by cohesin and PcG proteins. This is supported by three results: Wapl colocalizes with the cohesin subunit Rad21 on polytene chromosome; *wapl*^{AG} interferes with the function of PcG-silencing at specific targets; and *wapl*^{AG} phenotypes are modified by mutations in *Nipped-B* and *pds5*, two cohesin-associated factors.

wapl-null mutants die as third instar larvae and are germline lethal. By contrast, *wapl*^{AG} mutants live until the pharate adult stage and germline clones are viable. *wapl*^{AG} is a mutation that introduces a stop codon in the Wapl-L transcription unit, leaving the Wapl-S transcription unit intact. Wapl-L is transcribed throughout development, whereas Wapl-S is transcribed at all times except in larvae. We suggest that the lethality of *wapl*^{AG} results

from a loss in total Wapl levels owing to the absence of expression of Wapl-S in larvae, and that Wapl-S is sufficient for germline development. What about the dominant effect of *wapl*^{AG}? We suggest that the N-terminal region of the Wapl-L protein plays a regulatory role that attenuates the activity of Wapl and that the presence of Wapl-AG, coupled with the loss of the Wapl-L C terminus, leads to an attenuation of Wapl activity in *wapl*^{AG} mutants. The rescue of both the lethality and the extra-sex combs phenotype of *wapl*^{AG} by *UAS-Wapl-S* is consistent with this hypothesis. Overproduction of Wapl-AG using the Gal4 system would similarly attenuate Wapl activity leading to disrupted gene expression of cohesin-regulated genes.

We do not know how Wapl-AG interferes with Wapl function. The colocalization of Wapl-AG with Rad21 on polytene chromosomes suggests that it might interact with either wild-type Wapl or its interacting partner Pds5. The amino acid sequence FGF is important for the interaction of human Wapl with human Pds5 (Shintomi and Hirano, 2009), but this sequence is not present in either Wapl-S or Wapl-L. Protein structure and domain prediction programs did not find any distinguishing features in the N-terminal sequence of Wapl-L. Comparison of the amino acid sequence of Wapl-AG and Wapl-S showed a number of short stretches of sequence identity, and, curiously, one of our polyclonal α -Wapl-L antibodies, which was not used in these studies, recognized overexpressed Wapl-S protein weakly, suggesting that the antigens used for the two immunizations might share some epitopes. Clearly, more work needs to be done to determine how Wapl-AG disrupts cohesin function.

If Wapl is important for removing cohesin from the chromosomes, why does it colocalize with it on polytene chromosomes? Cohesin binding is dynamic (Gause et al., 2010). Our results show that interfering with Wapl function causes an increase in cohesin-binding stability. Our results suggest that Wapl probably cycles on and off the chromosomes with cohesin. This is consistent with the finding that Pds5, the Wapl interaction partner, has virtually identical chromosome-binding dynamics as cohesin, including a stable-binding form with a long chromosomal residence time (Gause et al., 2010).

Cohesin binding occurs mainly at transcriptionally active genes with paused polymerase, and with rare exceptions, is not detectable at PcG-silenced genes marked by H3K27me3 (Fay et al., 2011; Misulovin et al., 2008). Our data show that Wapl-AG increases both the stability and extent of cohesin binding, and therefore suggest that stronger cohesin binding interferes with the function of PcG proteins at silenced genes. We theorize, therefore, that cohesin may be actively excluded from silenced genes. In the rare cases where cohesin binding overlaps H3K27me3, the genes are

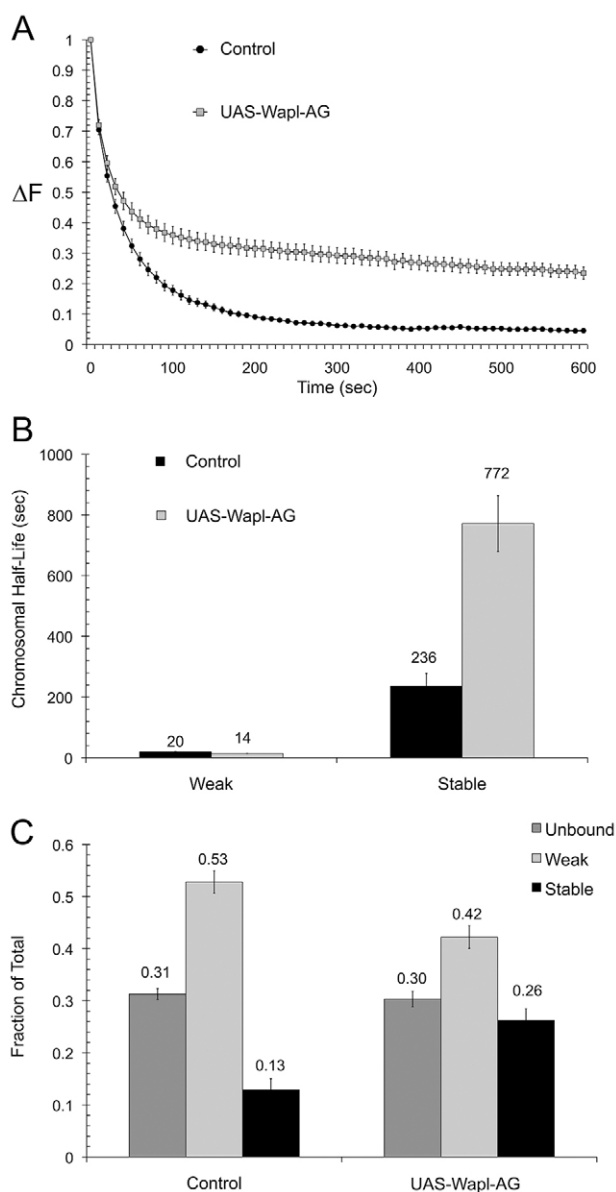


Fig. 7. Wapl-AG increases the stability of cohesin binding to polytene chromosomes. (A) FRAP recovery curves of EGFP-Smc1 (cohesin) after photobleaching of control salivary gland nuclei and salivary nuclei expressing Wapl-AG. The curves show the decreasing difference in fluorescence (ΔF) between the unbleached and bleached halves of the nuclei over time. Each curve is the average of ~ 30 nuclei. (B) The chromosomal half-lives of the weak and stable binding forms of cohesin (EGFP-Smc1) derived from a two-binding mode model (Gause et al., 2010) of the FRAP recovery curves. (C) Distribution of cohesin (EGFP-Smc1) into unbound, weakly bound and stably bound fractions derived from the FRAP recovery curves using the two binding mode model. The amount of unbound cohesin is determined from the loss of fluorescence in the unbleached half of the nucleus upon photobleaching. Error bars in all panels indicate the s.e.m.

not fully silenced (Schaaf et al., 2009). Although this is consistent with the idea that cohesin counteracts silencing, in fact cohesin negatively regulates expression in these unusual cases, in part by blocking transition of paused RNA polymerase to elongation (Fay et al., 2011). The complex interplay between cohesin and PcG proteins revealed by these and prior studies show that cohesin

Table 2. Nondisjunction in *wapl^{AG}* germline clones

Genotype*	Progeny scored	y ⁺ sons [†]	ci progeny [‡]
y <i>wapl^{AG} FRT</i>	1956	6	5
y <i>FRT</i>	1790	0	2

*For full genotype, see Materials and methods.

[†]X-chromosome non-disjunction.

[‡]Fourth chromosome non-disjunction.

regulates gene expression by additional mechanisms beyond its long-recognized role in facilitating enhancer-promoter interactions (Dorsett, 2011).

It is worth noting that the phenotypes we see with *wapl^{AG}* are very specific, and overlap those seen with reduction in the dose of PcG proteins, suggesting that the target genes that are the most sensitive to PcG activity are also the most sensitive to cohesin. The extra sex combs phenotype seen in *wapl^{AG}* mutants is the defining feature of PcG group genes (Kennison, 1995). It is caused by the loss of *Scr* silencing, which is exquisitely sensitive to the level of PcG proteins. Strictly speaking, *wapl^{AG}* can be classified as a PcG mutation. Interestingly, mutations in both *Nipped-B* and *vtd*, which codes for Rad21, have been classified as trxG genes. In fact, *vtd* mutations were first isolated as suppressors of the extra sex combs phenotype caused by *Polycomb* mutations (Kennison and Tamkun, 1988). Therefore, trxG phenotypes can be caused by mutations in cohesin subunits, whereas PcG phenotypes can be caused by mutations that increase cohesin binding. Our data further suggest that increasing cohesin stability can inhibit PcG function by interfering with interactions between PREs. A 181 bp minimal *engrailed* PRE can repress *mini-white* expression in a transgene when present as a single copy (in flies heterozygous for the transgene), but it is much more effective when present in two copies (in flies homozygous for the transgene) (Noyes et al., 2011). *wapl^{AG}* affects only the eye color of homozygous flies, suggesting that it only acts on paired PREs. Interestingly, control of *Scr* also depends on interactions between regulatory elements, most probably PREs (Southworth and Kennison, 2002). These data, combined with data showing a biochemical interaction between cohesin and PcG proteins (Strübbe et al., 2011), suggest that cohesin might directly inhibit PcG function.

Acknowledgements

We thank Payal Ray and Sandip De for comments on the manuscript and the Bloomington Stock Center for fly stocks.

Funding

This research was supported by the National Institutes of Health (NIH) [R01 GM055683 to D.D. and M.G.] and by the Intramural Research Program of the National Institute of Child Health and Human Development, NIH. Deposited in PMC for release after 12 months.

Competing interests statement

The authors declare no competing financial interests.

Supplementary material

Supplementary material available online at <http://dev.biologists.org/lookup/suppl/doi:10.1242/dev.084566/-/DC1>

References

- Chou, T. B. and Perrimon, N. (1996). The autosomal FLP-DFS technique for generating germline mosaics in *Drosophila melanogaster*. *Genetics* **144**, 1673-1679.
- Dorsett, D. (2011). Cohesin: genomic insights into controlling gene transcription and development. *Curr. Opin. Genet. Dev.* **21**, 199-206.
- Eisenberg, J. C. (2006). Functional genomics of histone modification and non-histone chromosomal proteins using the polytene chromosomes of *Drosophila*. *Methods* **40**, 360-364.

- Fay, A., Misulovin, Z., Li, J., Schaaf, C. A., Gause, M., Gilmour, D. S. and Dorsett, D. (2011). Cohesin selectively binds and regulates genes with paused RNA polymerase. *Curr. Biol.* **21**, 1624-1634.
- Gandhi, R., Gillespie, P. J. and Hirano, T. (2006). Human Wapl is a cohesin-binding protein that promotes sister-chromatid resolution in mitotic prophase. *Curr. Biol.* **16**, 2406-2417.
- Gause, M., Misulovin, Z., Bilyeu, A. and Dorsett, D. (2010). Dosage-sensitive regulation of cohesin chromosome binding and dynamics by Nipped-B, Pds5, and Wapl. *Mol. Cell. Biol.* **30**, 4940-4951.
- Hallson, G., Syrzycka, M., Beck, S. A., Kennison, J. A., Dorsett, D., Page, S. L., Hunter, S. M., Keall, R., Warren, W. D., Brock, H. W. et al. (2008). The Drosophila cohesin subunit Rad21 is a trithorax group (trxG) protein. *Proc. Natl. Acad. Sci. USA* **105**, 12405-12410.
- Kassis, J. A. (1994). Unusual properties of regulatory DNA from the Drosophila engrailed gene: three "pairing-sensitive" sites within a 1.6-kb region. *Genetics* **136**, 1025-1038.
- Kassis, J. A. (2002). Pairing-sensitive silencing, polycomb group response elements, and transposon homing in Drosophila. *Adv. Genet.* **46**, 421-438.
- Kennison, J. A. (1995). The Polycomb and trithorax group proteins of Drosophila: trans-regulators of homeotic gene function. *Annu. Rev. Genet.* **29**, 289-303.
- Kennison, J. A. and Tamkun, J. W. (1988). Dosage-dependent modifiers of polycomb and antennapedia mutations in Drosophila. *Proc. Natl. Acad. Sci. USA* **85**, 8136-8140.
- Kerppola, T. K. (2009). Polycomb group complexes – many combinations, many functions. *Trends Cell Biol.* **19**, 692-704.
- Kueng, S., Hegemann, B., Peters, B. H., Lipp, J. J., Schleiffer, A., Mechtler, K. and Peters, J.-M. (2006). Wapl controls the dynamic association of cohesin with chromatin. *Cell* **127**, 955-967.
- Kwon, D., Mucci, D., Langlais, K. K., Americo, J. L., DeVido, S. K., Cheng, Y. and Kassis, J. A. (2009). Enhancer-promoter communication at the Drosophila engrailed locus. *Development* **136**, 3067-3075.
- McQuilton, P., St Pierre, S. E., Thurmond, J. and the FlyBase Consortium (2012). FlyBase 101 – the basics of navigating FlyBase. *Nucleic Acids Res.* **40** Database issue, D706-D714.
- Misulovin, Z., Schwartz, Y. B., Li, X. Y., Kahn, T. G., Gause, M., MacArthur, S., Fay, J. C., Eisen, M. B., Pirrotta, V., Biggin, M. D. et al. (2008). Association of cohesin and Nipped-B with transcriptionally active regions of the Drosophila melanogaster genome. *Chromosoma* **117**, 89-102.
- Müller, J. and Kassis, J. A. (2006). Polycomb response elements and targeting of polycomb group proteins in Drosophila. *Curr. Opin. Genet. Dev.* **16**, 476-484.
- Müller, J. and Verrijzer, P. (2009). Biochemical mechanisms of gene regulation by polycomb group protein complexes. *Curr. Opin. Genet. Dev.* **19**, 150-158.
- Nasmyth, K. (2011). Cohesin: a catenase with separate entry and exit gates? *Nat. Cell Biol.* **13**, 1170-1177.
- Noyes, A., Stefaniuk, C., Cheng, Y., Kennison, J. A. and Kassis, J. A. (2011). Modulation of the activity of a polycomb-group response element in Drosophila by a mutation in the transcriptional activator Woc. *G3* **1**, 471-478.
- Perrimon, N., Engstrom, L. and Mahowald, A. P. (1985). Developmental genetics of the 2C-D region of the Drosophila X chromosome. *Genetics* **111**, 23-41.
- Peters, J.-M., Tedeschi, A. and Schmitz, J. (2008). The cohesin complex and its roles in chromosome biology. *Genes Dev.* **22**, 3089-3114.
- Ringrose, L. and Paro, R. (2007). Polycomb/Trithorax response elements and epigenetic memory of cell identity. *Development* **134**, 223-232.
- Schaaf, C. A., Misulovin, Z., Sahota, G., Siddiqui, A. M., Schwartz, Y. B., Kahn, T. G., Pirrotta, V., Gause, M. and Dorsett, D. (2009). Regulation of the Drosophila enhancer of split and invected-engrailed gene complexes by sister chromatid cohesion proteins. *PLoS ONE* **4**, e6202.
- Shintomi, K. and Hirano, T. (2009). Releasing cohesin from chromosome arms in early mitosis: opposing actions of Wapl-Pds5 and Sgo1. *Genes Dev.* **23**, 2224-2236.
- Simon, J. A. and Kingston, R. E. (2009). Mechanisms of polycomb gene silencing: knowns and unknowns. *Nat. Rev. Mol. Cell Biol.* **10**, 697-708.
- Southworth, J. W. and Kennison, J. A. (2002). Transvection and silencing of the Scr homeotic gene of Drosophila melanogaster. *Genetics* **161**, 733-746.
- Strübbe, G., Popp, C., Schmidt, A., Pauli, A., Ringrose, L., Beisel, C. and Paro, R. (2011). Polycomb purification by in vivo biotinylation tagging reveals cohesin and Trithorax group proteins as interaction partners. *Proc. Natl. Acad. Sci. USA* **108**, 5572-5577.
- Sutani, T., Kawaguchi, T., Kanno, R., Itoh, T. and Shirahige, K. (2009). Budding yeast Wpl1(Rad61)-Pds5 complex counteracts sister chromatid cohesion-establishing reaction. *Curr. Biol.* **19**, 492-497.
- Verni, F., Gandhi, R., Goldberg, M. L. and Gatti, M. (2000). Genetic and molecular analysis of wings apart-like (wapl), a gene controlling heterochromatin organization in Drosophila melanogaster. *Genetics* **154**, 1693-1710.
- Xiong, B. and Gerton, J. L. (2010). Regulators of the cohesin network. *Annu. Rev. Biochem.* **79**, 131-153.

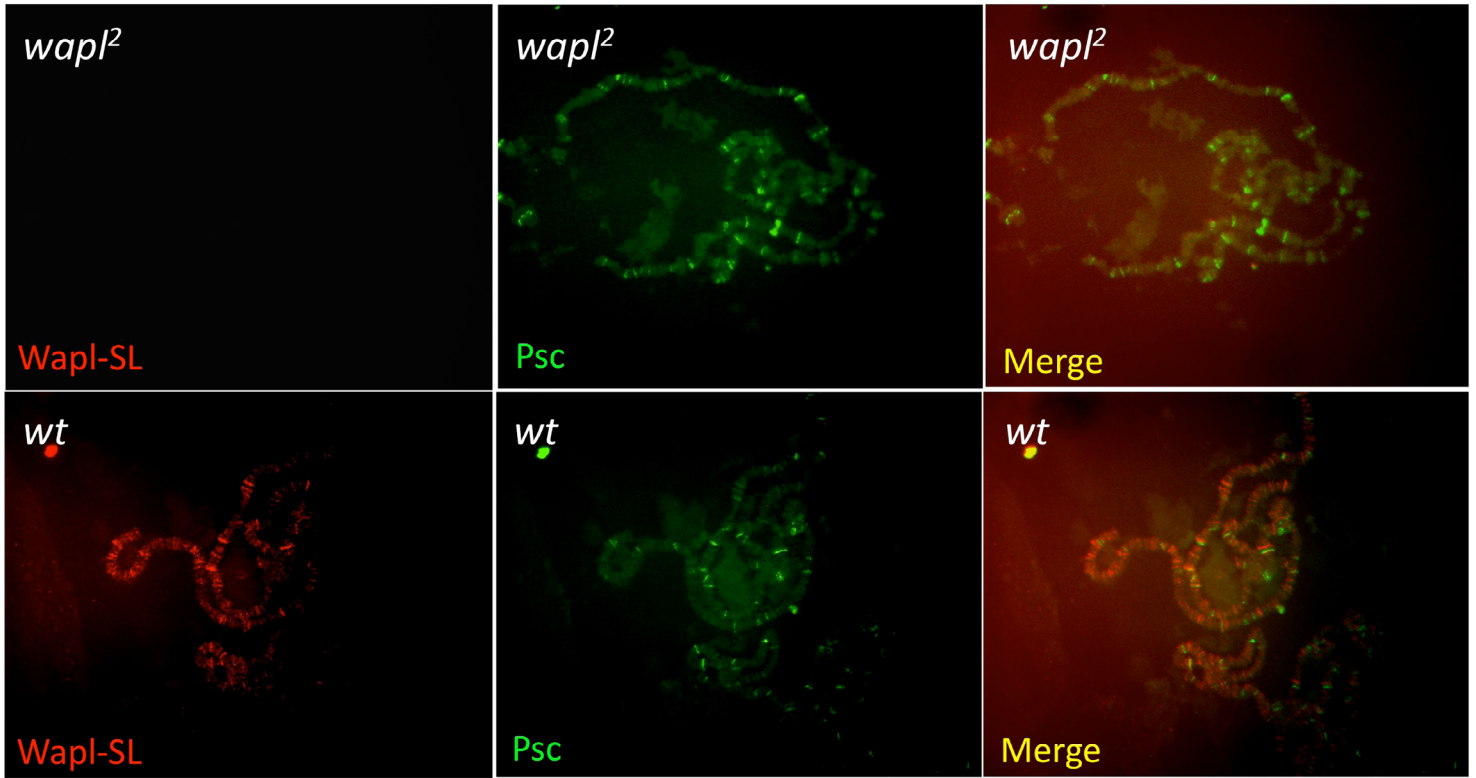


Fig. S1. Wapl-SL antigen is not present in *wapl*² mutants. Polytene chromosomes from wild-type (*wt*) and *wapl*² larvae were co-stained with α -Wapl-SL (affinity-purified, 1:50, Red) and α -Psc (monoclonal, 1:25, green). No Wapl-SL antigen is visible in *wapl*² mutants. Wapl and Psc largely do not colocalize. Similar results were obtained for the colocalization of Pc and Rad21 on polytene chromosomes (Strübbe et al., 2011).

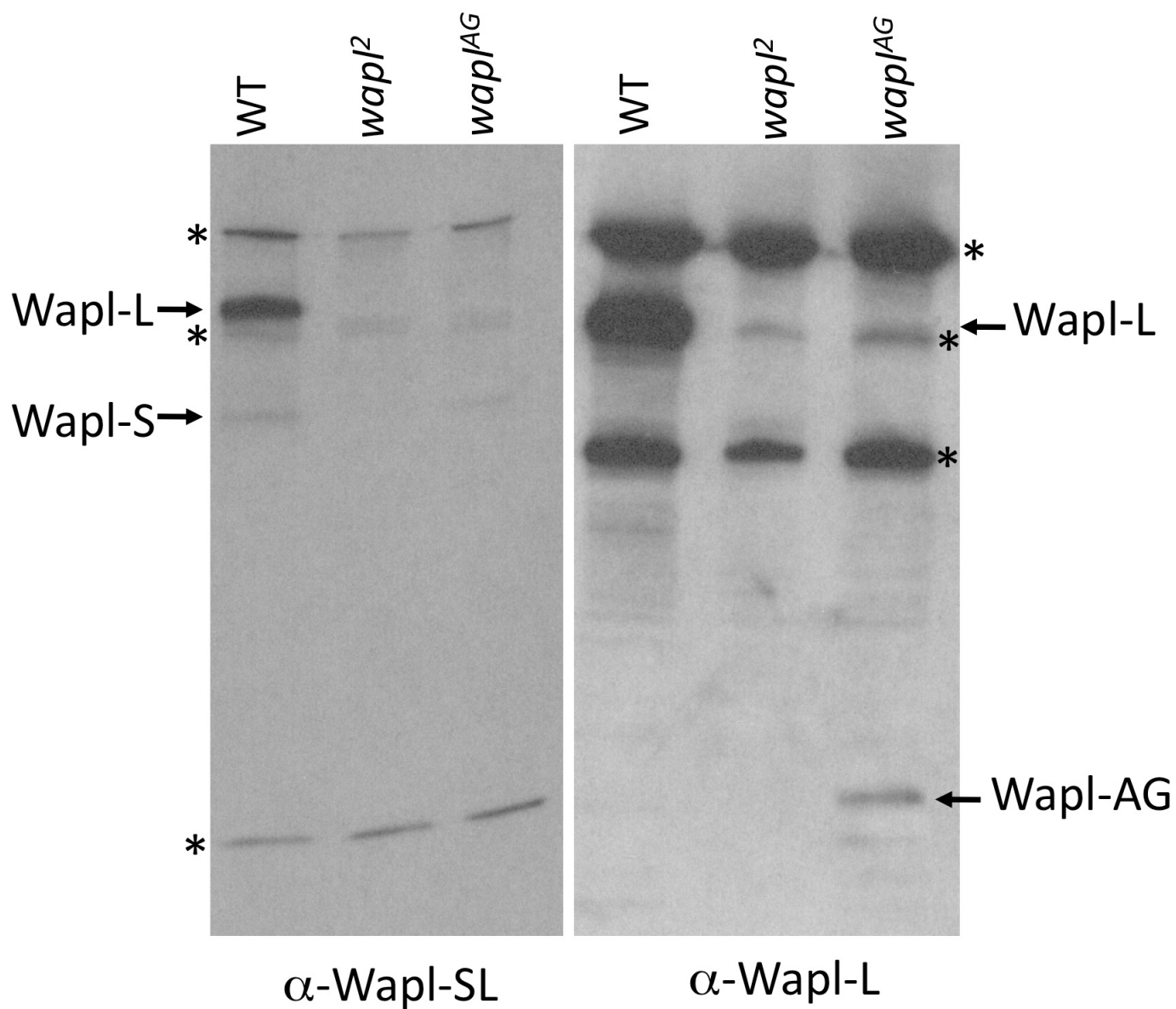


Fig. S2. Larval western blots with α -Wapl-SL and α -Wapl-L antisera. Protein extracts from larvae of the genotypes wild type, *wapl*² and *wapl*^{AG} were subjected to SDS-electrophoresis and western blotting and probed with either α -Wapl-SL or α -Wapl-L. Part of this α -Wapl-SL blot is shown in Fig. 3C. Asterisks mark crossreacting bands.